



Supplement of

Contrasting projections of the ENSO-driven CO₂ flux variability in the equatorial Pacific under high-warming scenario

Pradeebane Vaithinada Ayar et al.

Correspondence to: Pradeebane Vaithinada Ayar, (paya@norceresearch.no, pradeebane@laposte.net)

The copyright of individual parts of the supplement might differ from the article licence.

Stratification Index

To compute Stratification Index, in situ density (ρ) has been calculated from each ESM's potential temperature and practical salinity (after conversion to absolute salinity and conservative temperature) following TEOS-10 standards (Feistel, 2008) and using R “gsw” (<https://cran.r-project.org/web/packages/gsw/index.html>). Three-dimensional ρ fields have been area-weighted over the EP region. We use a Stratification Index (SI) based on Sgubin et al. (2017) to characterise the stratification of the water column from surface to 500m:

$$SI = \sum_{i=1}^{25} \rho^{Z_i} - \rho^{Z_0}$$

where Z_0 is the sea surface and $Z_i = Z_{i-1} + 20$ and $i \in [1, \dots, 25]$.

References

- Feistel, R.: A Gibbs function for seawater thermodynamics for -6 to 80°C and salinity up to 120g kg⁻¹, Deep Sea Research Part I: Oceanographic Research Papers, 55, 1639–1671, <https://doi.org/https://doi.org/10.1016/j.dsr.2008.07.004>, 2008.
- Sgubin, G., Swingedouw, D., Drijfhout, S., Mary, Y., and Bennabi, A.: Abrupt cooling over the North Atlantic in modern climate models, Nature Communications, 8, <https://doi.org/https://doi.org/10.1038/ncomms14375>, 2017.

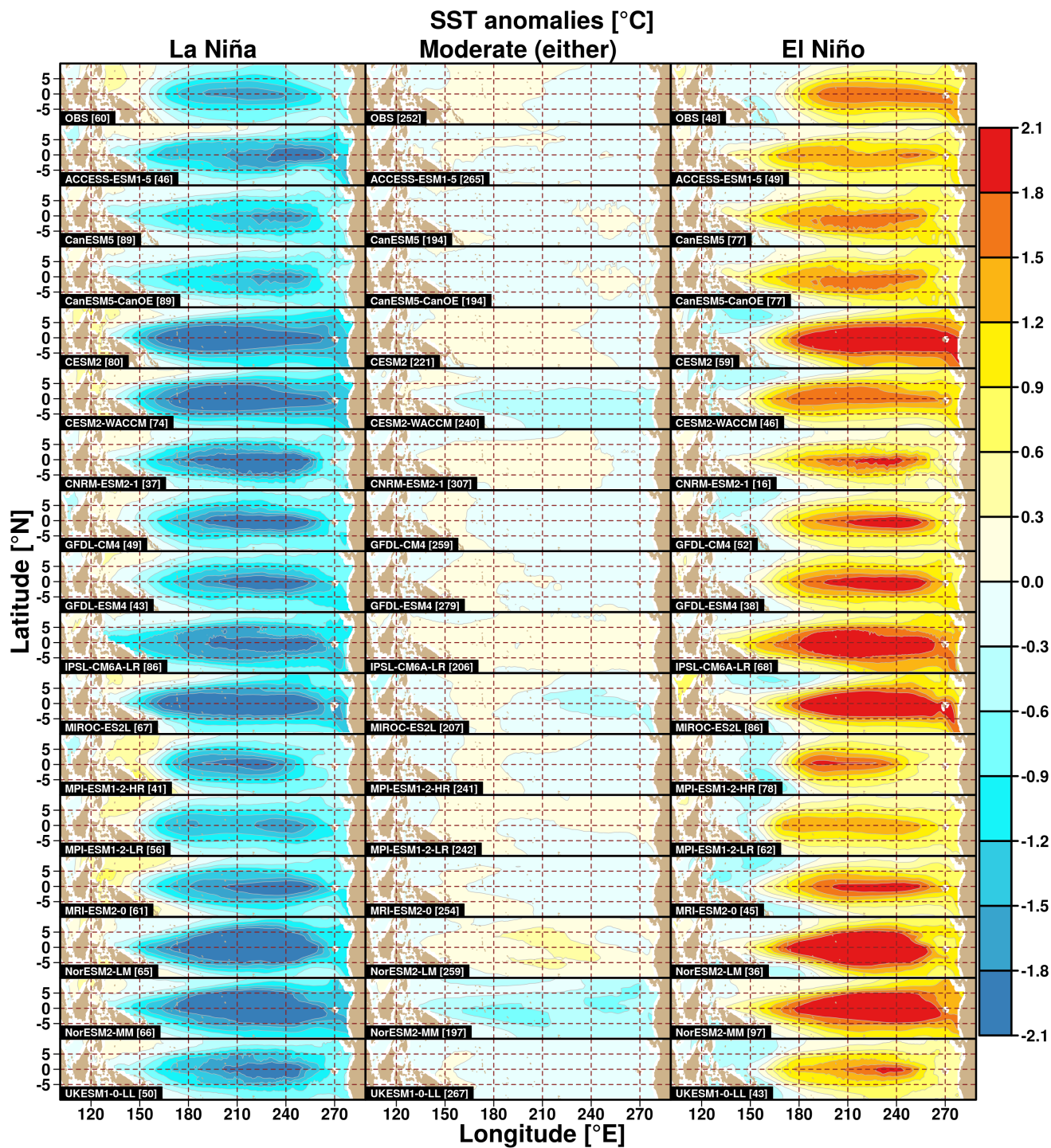


Figure S 1. CMIP6 ensemble SST (in °C) average anomalies over the 1985-2014 contemporary period for the La Niña, El Niño and the moderate regimes.

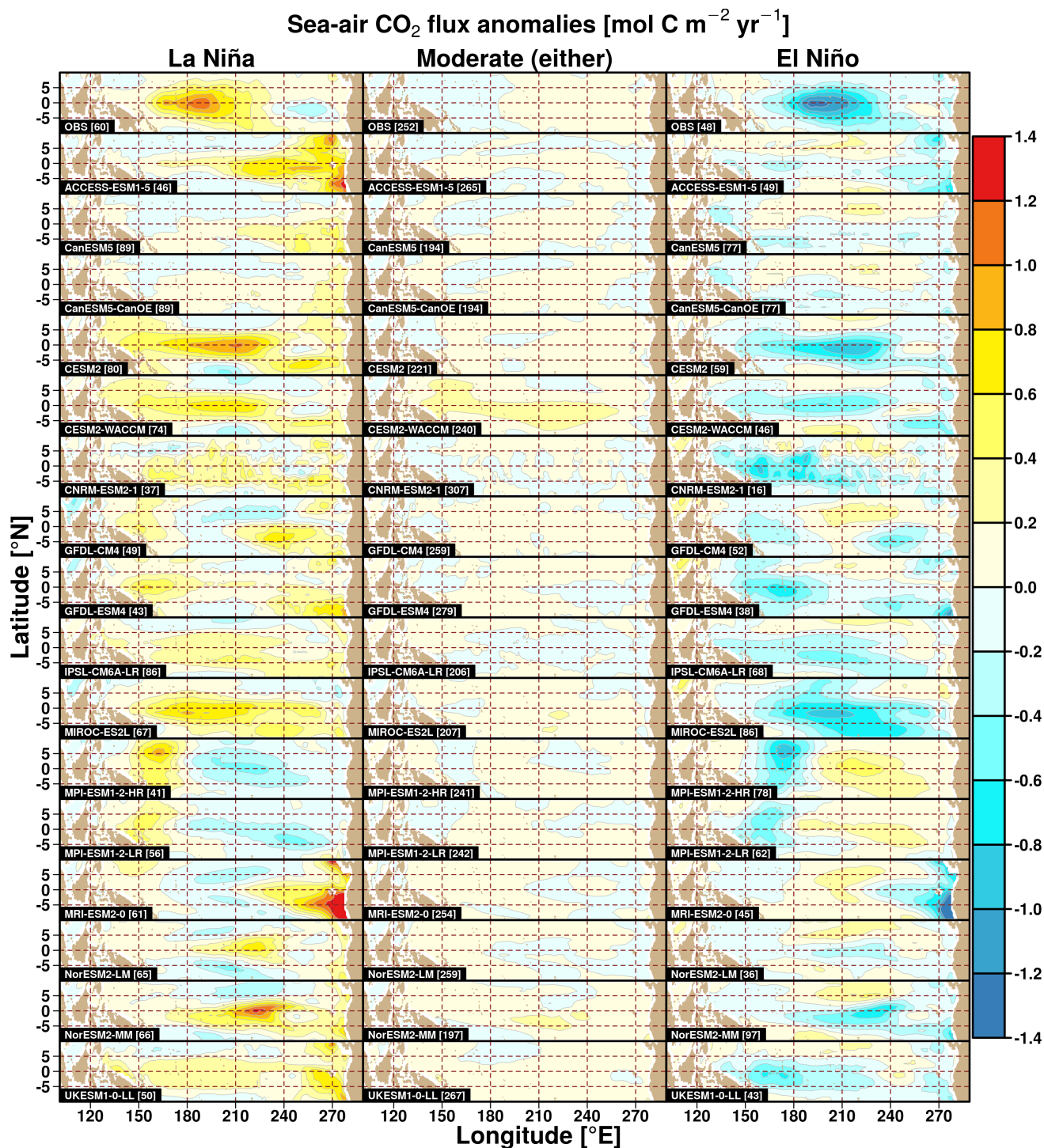


Figure S 2. CMIP6 ensemble sea-air CO₂ fluxes (in mol C m⁻² yr⁻¹) average anomalies over the 1985-2014 contemporary period for the La Niña, El Niño and the moderate regimes.

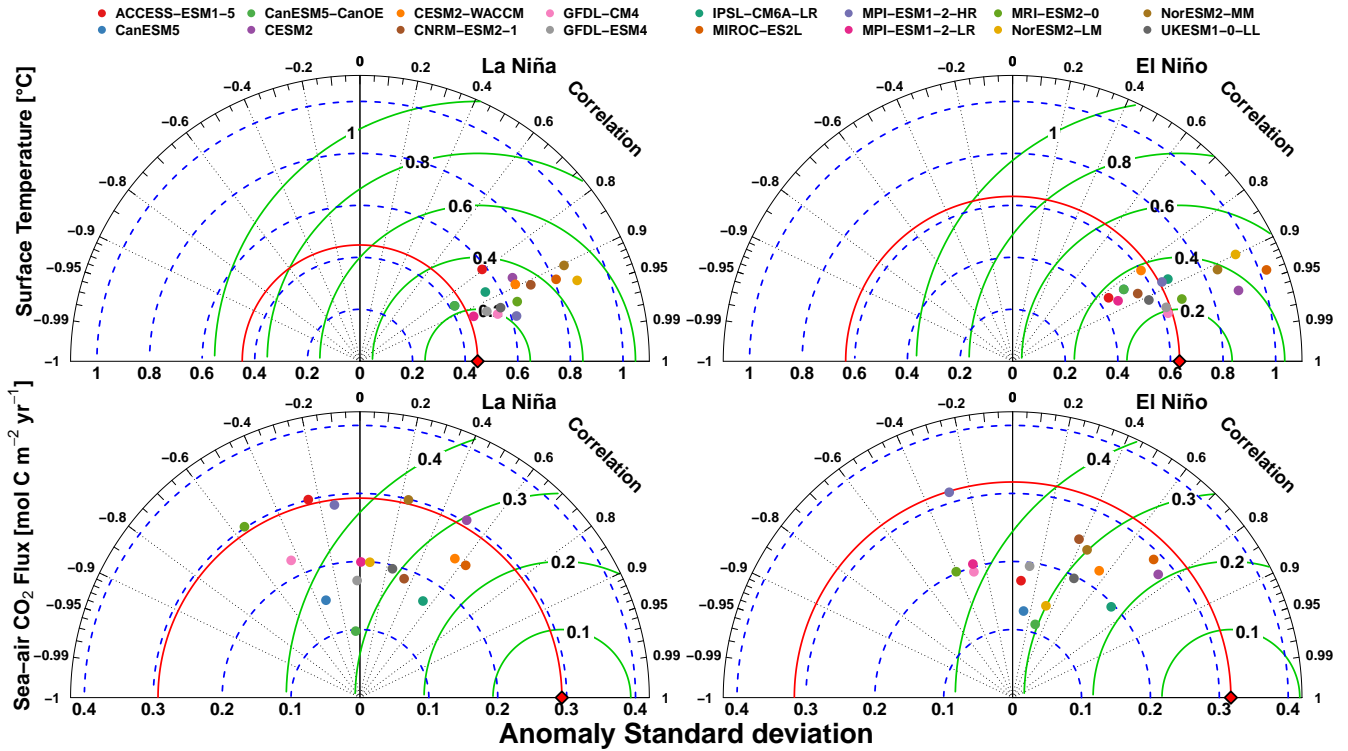


Figure S3. Taylor diagramme of CMIP6 ensemble SST (in °C, *top*) and sea-air CO₂ fluxes (in mol C m⁻² yr⁻¹, *bottom*) average anomalies over the 1985-2014 contemporary period for the La Niña and El Niño regimes. Reference values (observed mean values in our case) correspond to the red diamond on the abscissa. Radial distances from the origin are proportional to the standard deviation (blue dashed lines) while azimuthal positions give the correlation coefficient between the simulated and observed values. Finally the green circular lines correspond to the 'centred'-RMSE.

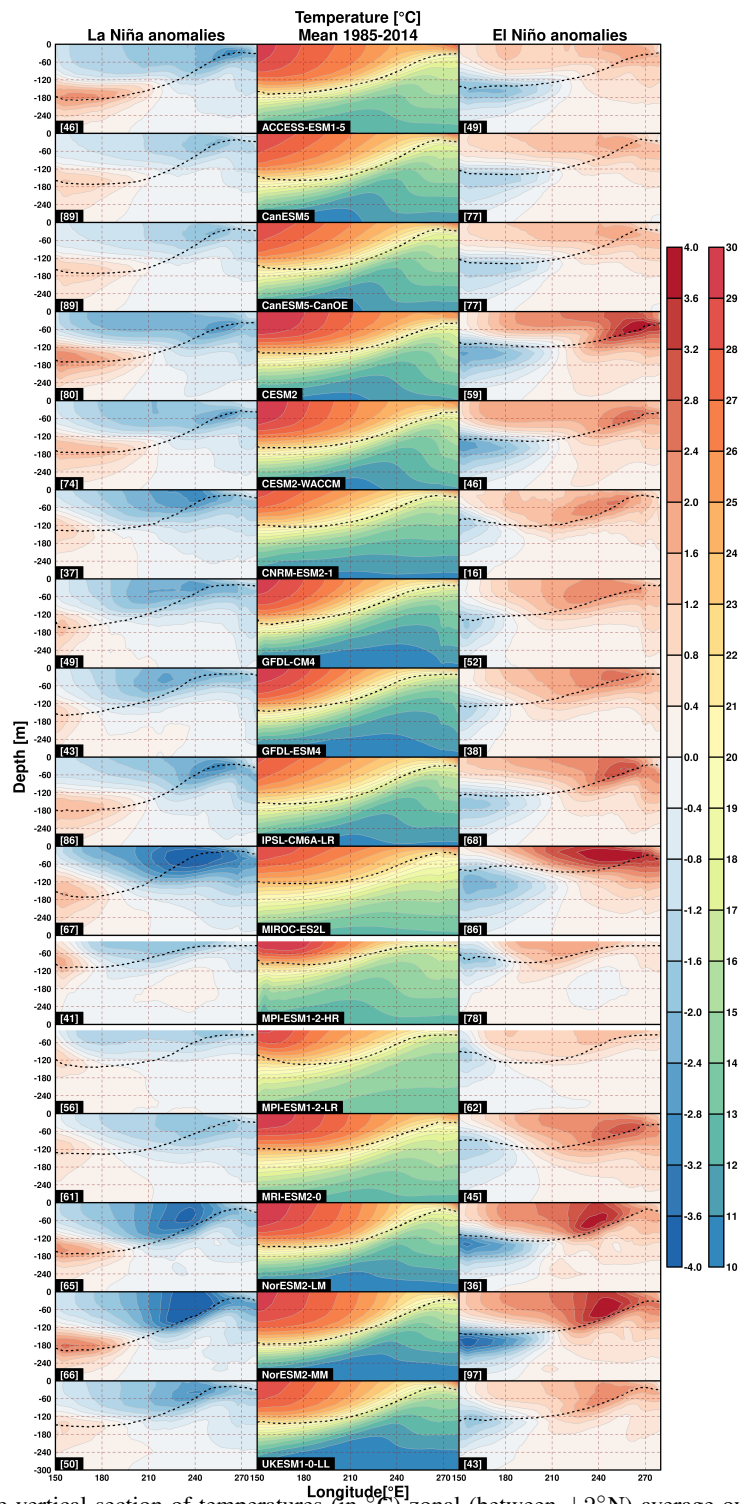


Figure S 4. CMIP6 ensemble vertical section of temperatures (in $^\circ\text{C}$) zonal (between $\pm 2^\circ\text{N}$) average over the 1985-2014 contemporary period (*middle*). Average anomalies (differences) relative to contemporary mean are given for La Niña (*left*) and El Niño (*right*) regimes. Dotted lines indicate the average thermocline depth. In square brackets, the number of months in each regime for each CMIP6 models.

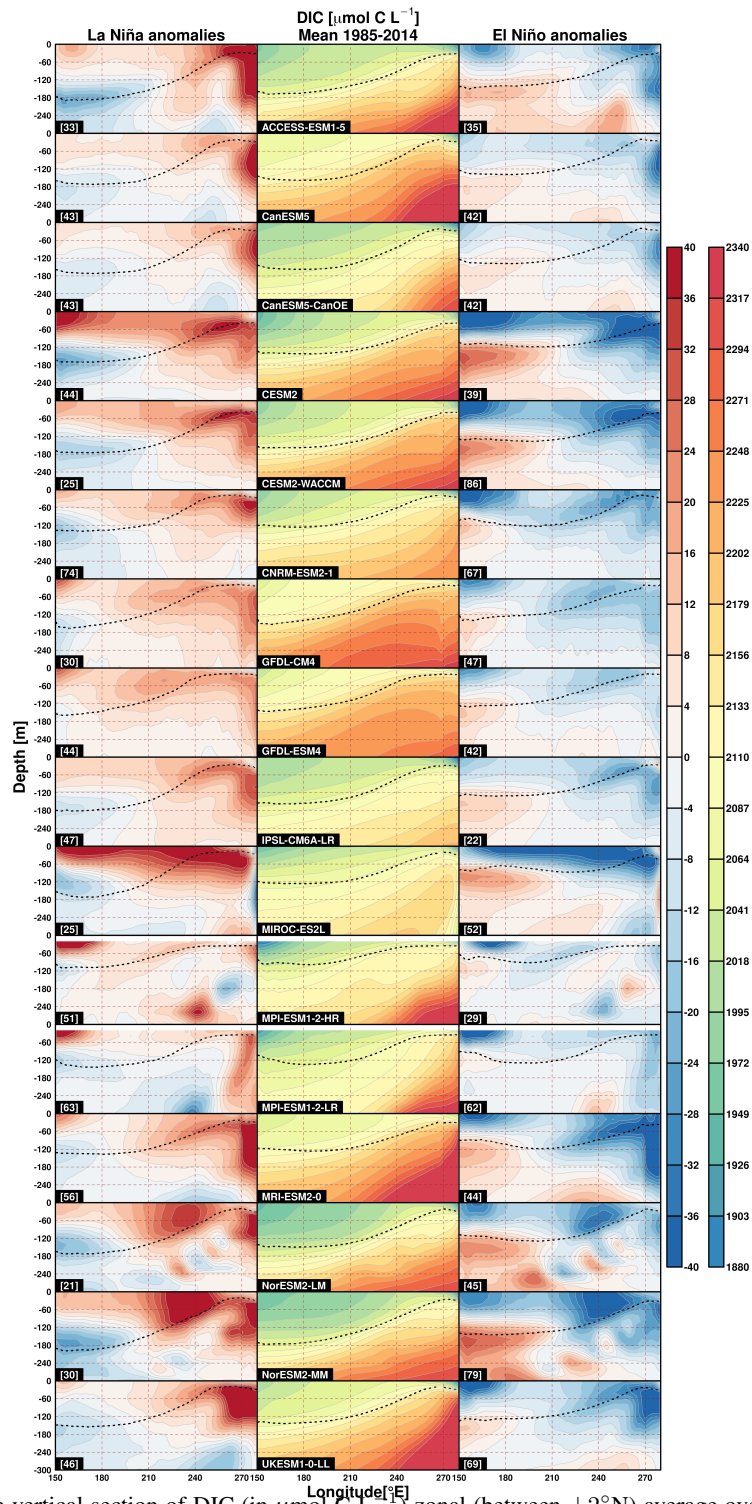


Figure S 5. CMIP6 ensemble vertical section of DIC (in $\mu\text{mol C L}^{-1}$) zonal (between $\pm 2^\circ\text{N}$) average over the 1985-2014 contemporary period (*middle*). Average anomalies (differences) relative to contemporary mean are given for La Niña (*left*) and El Niño (*right*) regimes. Dotted lines indicate the average thermocline depth. In square brackets, the number of months in each regimes for each CMIP6 models.

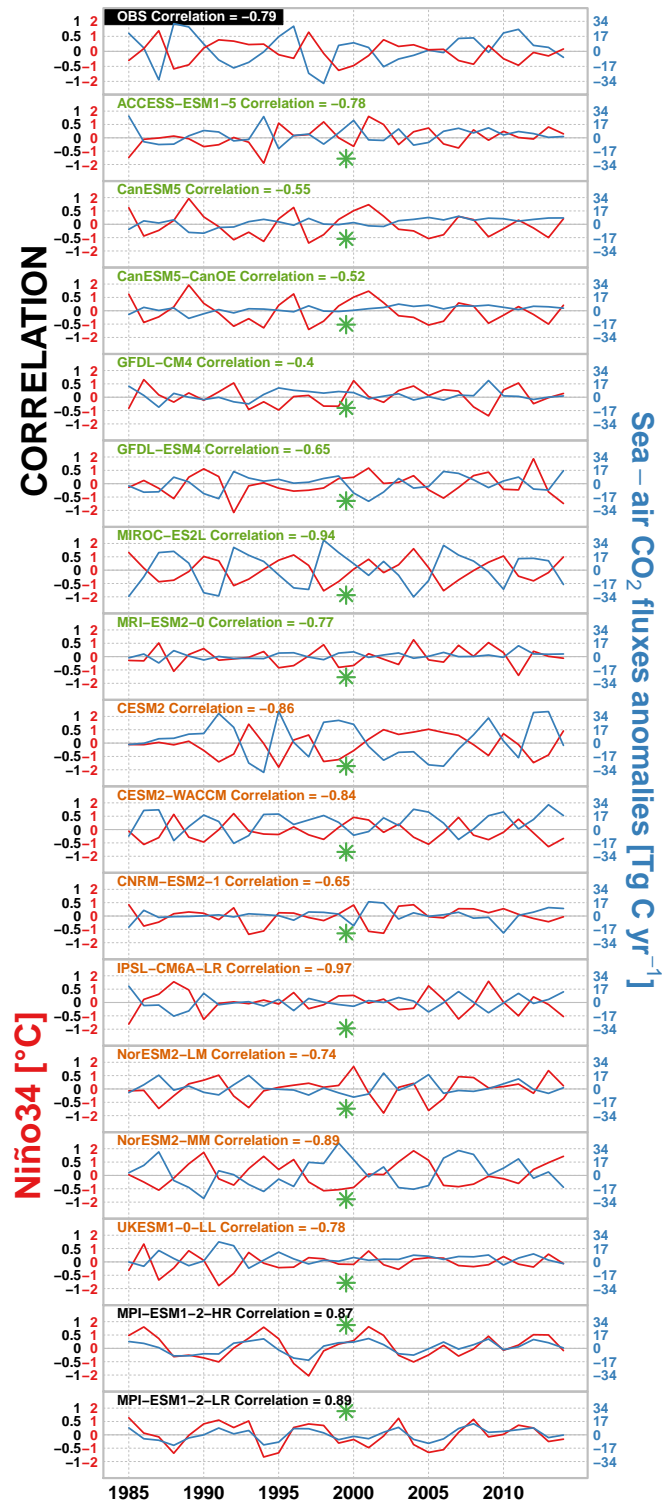


Figure S 6. Same as Figure 3 but for the 1985-2014 contemporary period.

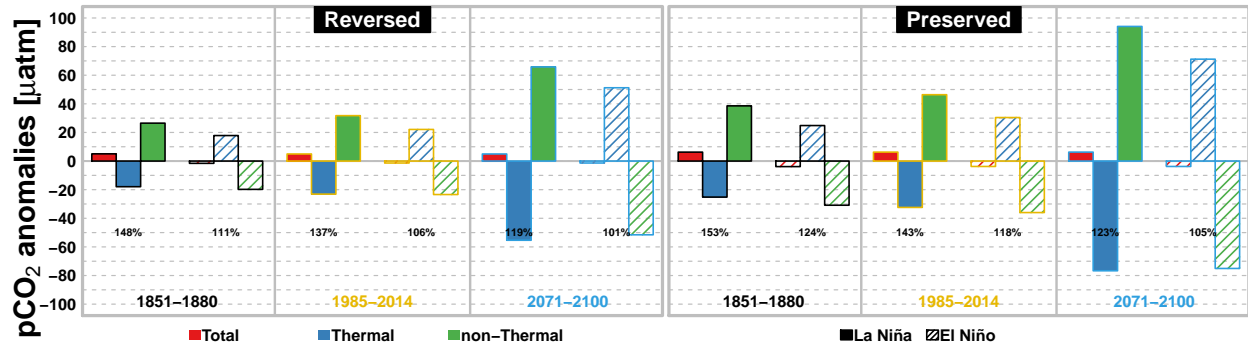


Figure S 7. El Niño and La Niña average of total (*in red*), thermal (*in blue*) and non-thermal (*in green*) $p\text{CO}_2$ mean anomalies (in μatm) for the reversed (*left*) and preserved (*right*) ESMs over the early historical (1851-1880) in EP domain. The same components are estimated by scaling the background $p\text{CO}_2$ scaled to contemporary (1985-2014) and future (2071-2100) periods. The absolute ratio between the non-thermal and thermal component is given (in %) for each periods, groups and ENSO phases.

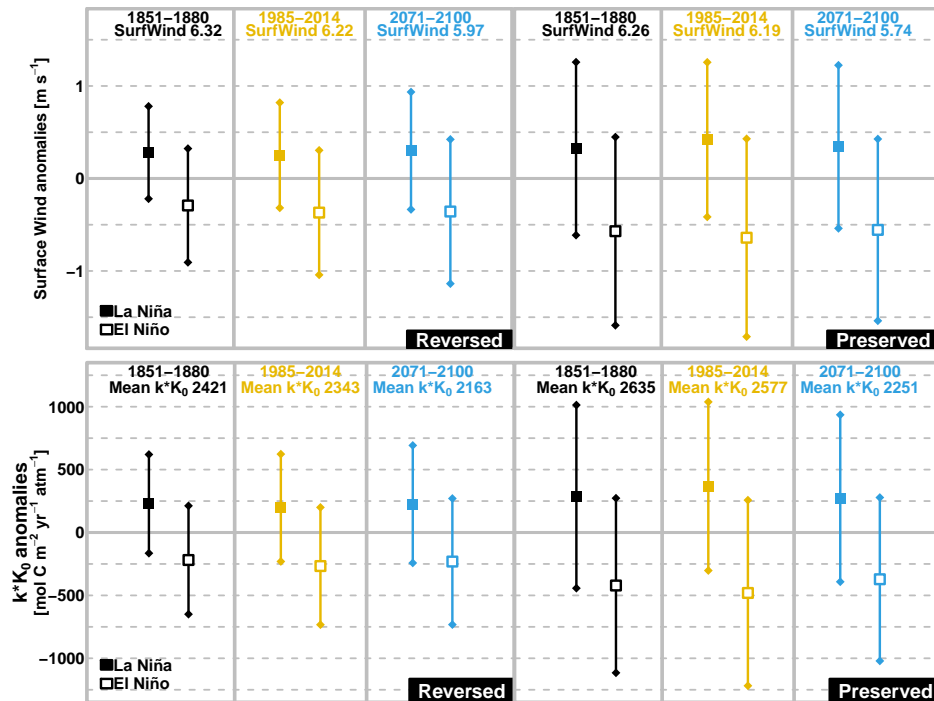


Figure S 8. El Niño and La Niña surface wind (*top* in m s^{-1}) and k^*K_0 (*bottom* in $\text{mol C m}^{-2} \text{yr}^{-2} \text{atm}^{-1}$) mean anomalies for the reversed (*left*) and preserved (*right*) ESMs over the early historical (1851-1880), contemporary (1985-2014) and future (2071-2100) periods in the EP domain. Vertical bars represents \pm one s.d. of the anomalies for the respective periods, groups of models and ENSO phases.

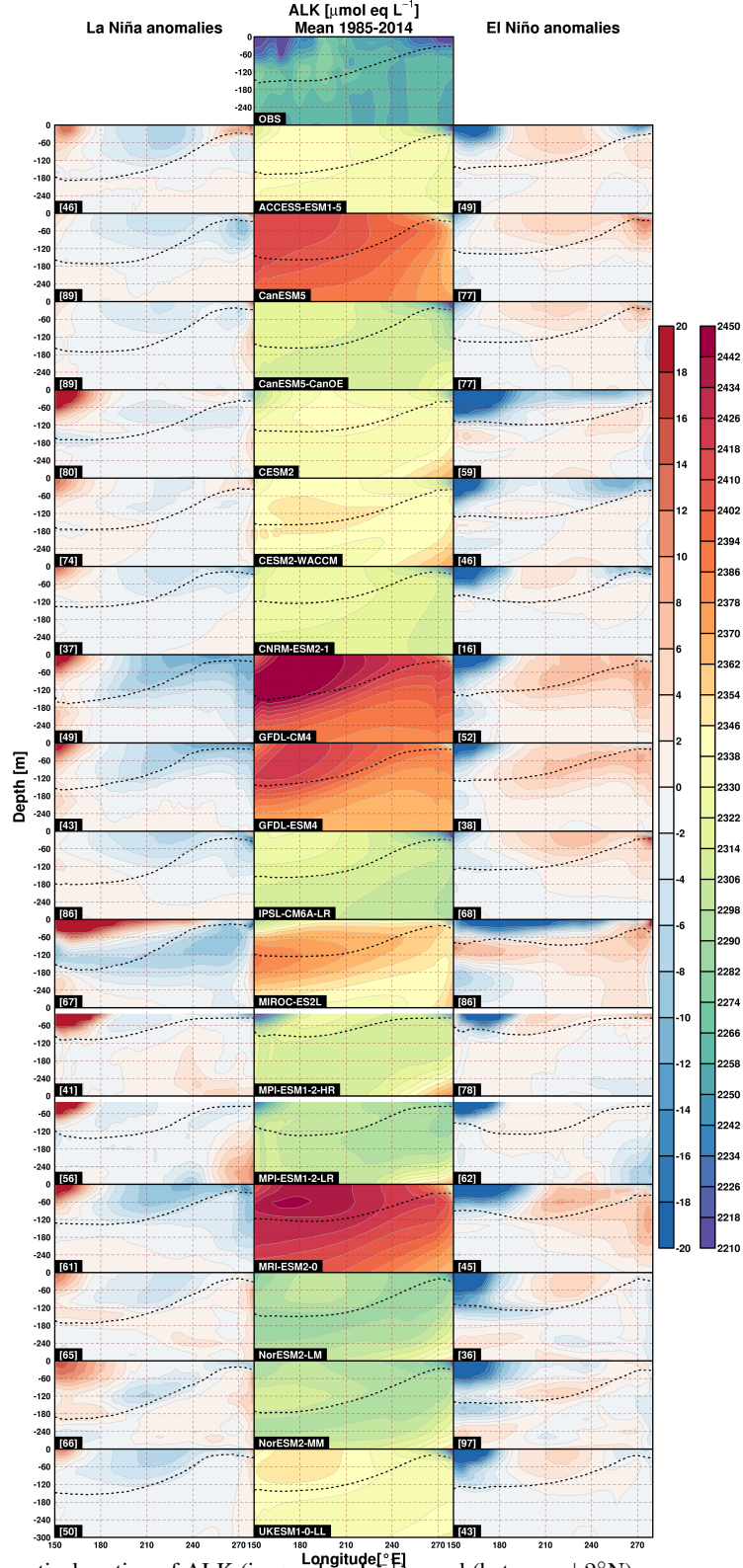


Figure S 9. CMIP6 ensemble vertical section of ALK (in $\mu\text{mol eq L}^{-1}$) zonal (between $\pm 2^\circ\text{N}$) average over the 1985-2014 contemporary period (*middle*). Average anomalies (differences) relative to contemporary mean are given for La Niña (*left*) and El Niño (*right*) regimes. Dotted lines indicate the average thermocline depth. In square brackets, the number of months in each regimes for each CMIP6 models.

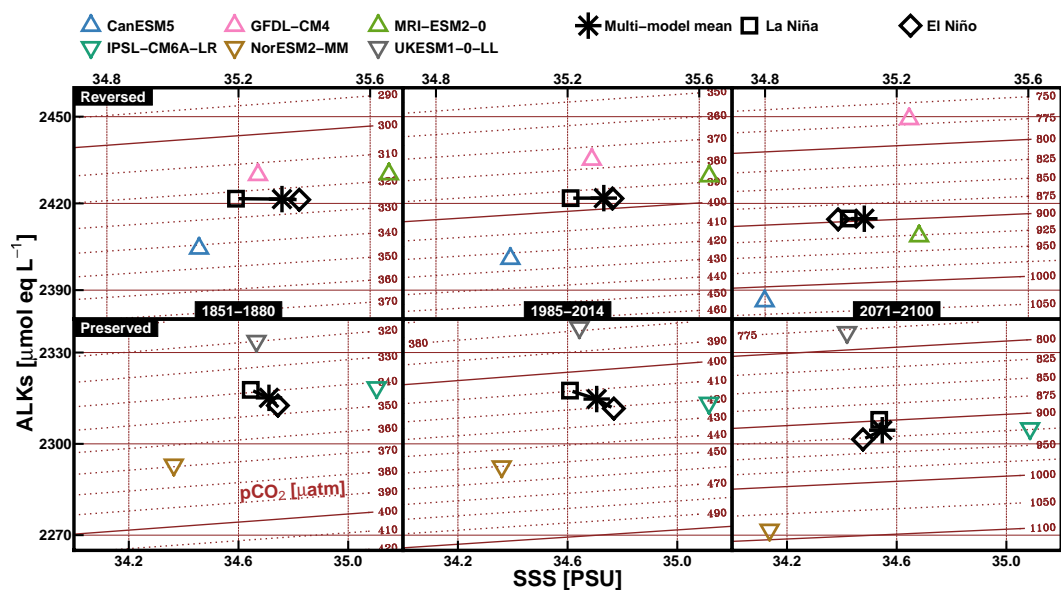


Figure S 10. Mean SSS (in psu) versus mean ALKs (in $\mu\text{mol eq L}^{-1}$) over the early historical (1851-1880), contemporary (1985-2014) and future (2071-2100) periods in the EP domain simulated by all reversed and preserved ESMs (*top* panels, circle markers). The multi-model mean values of SSS and ALK (asterisk markers) from each ESM group together with their respective mean values during La Niña (square markers) and El Niño (diamond markers) are also depicted for the three periods. Isopleths of $p\text{CO}_2$ for varying SSS and ALKs are given in the background and are computed from period and group specific SST and DICs multi-model average.

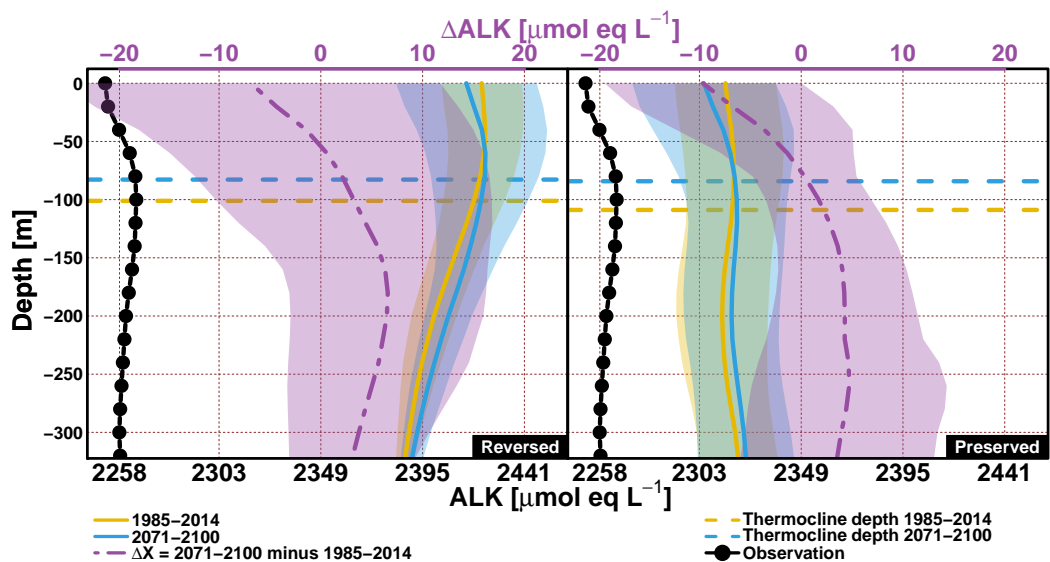


Figure S 11. Same as Fig.9 but for alkalinity.

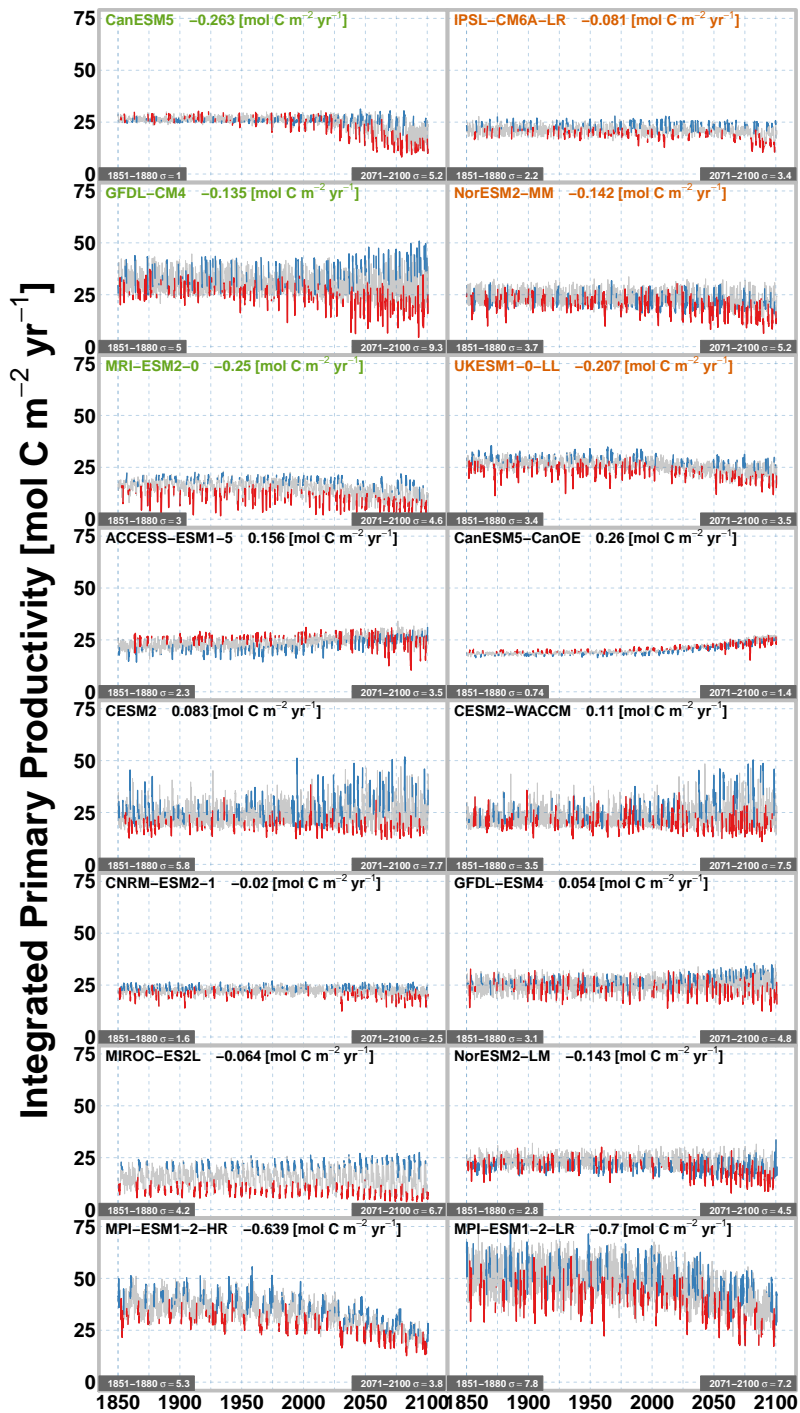


Figure S 12. Time-series of intPP (in $\text{mol C m}^{-2} \text{yr}^{-1}$) from 1850 to 2100. The blue and red colours indicates the occurrence of the La Niña and El Niño regimes. The decadal trend is given for each model. Models names are given in green for the selected models with shifting correlation sign, in orange for selected ones maintaining the negative correlation and black the others. The intPP standard deviation (σ) over the early historical (1851-1880) and future (2071-2100) periods are given for each model.

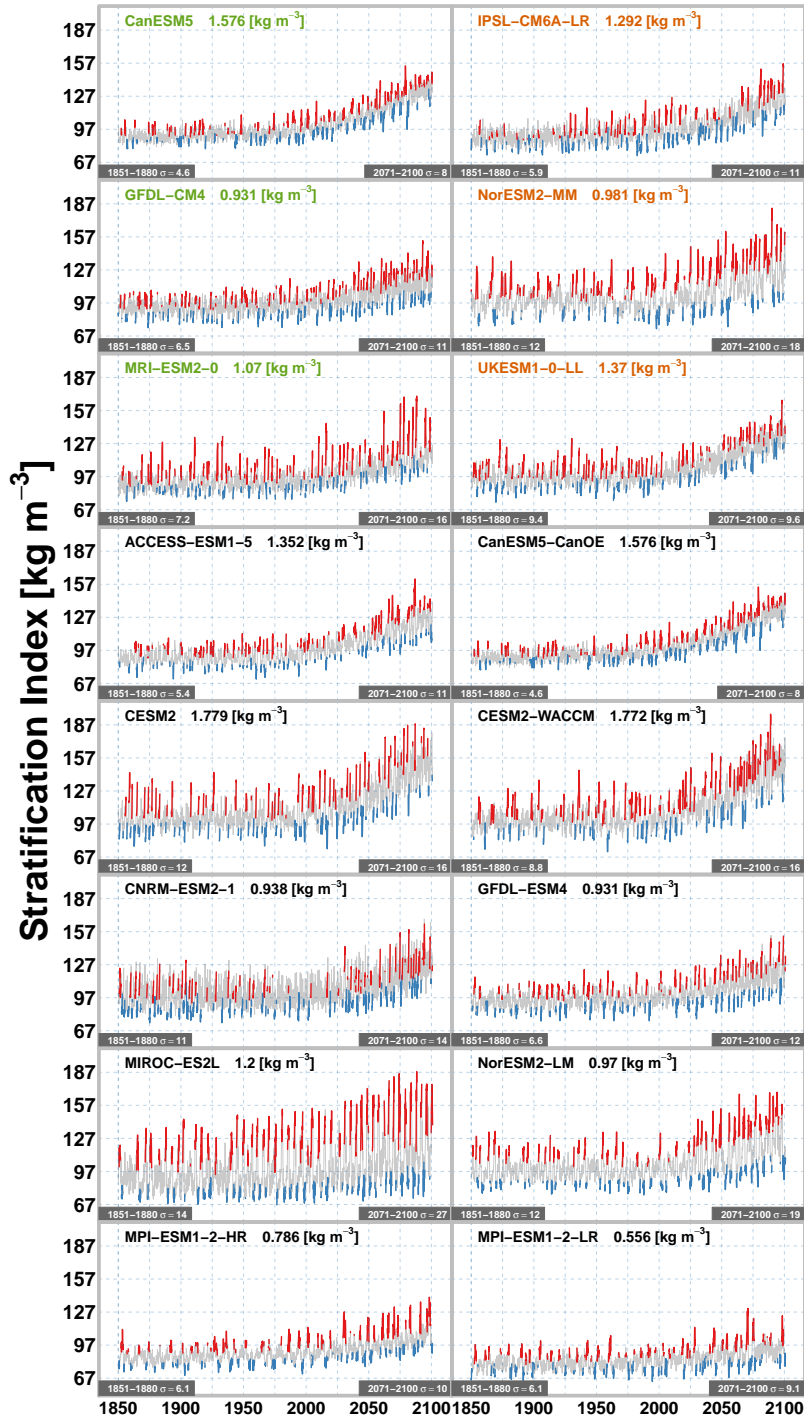


Figure S 13. Time-series of average SI (in kg m^{-3}) from 1885 to 2100. The blue and red colours indicates the occurrence of the La Niña and El Niño regimes. The decadal trend is given for each model. Models names are given in green for the selected models with shifting correlation sign, in orange for selected ones maintaining the negative correlation and black for the others. The SI standard deviation (σ) over the early historical (1851-1880) and future (2071-2100) periods are given for each model.

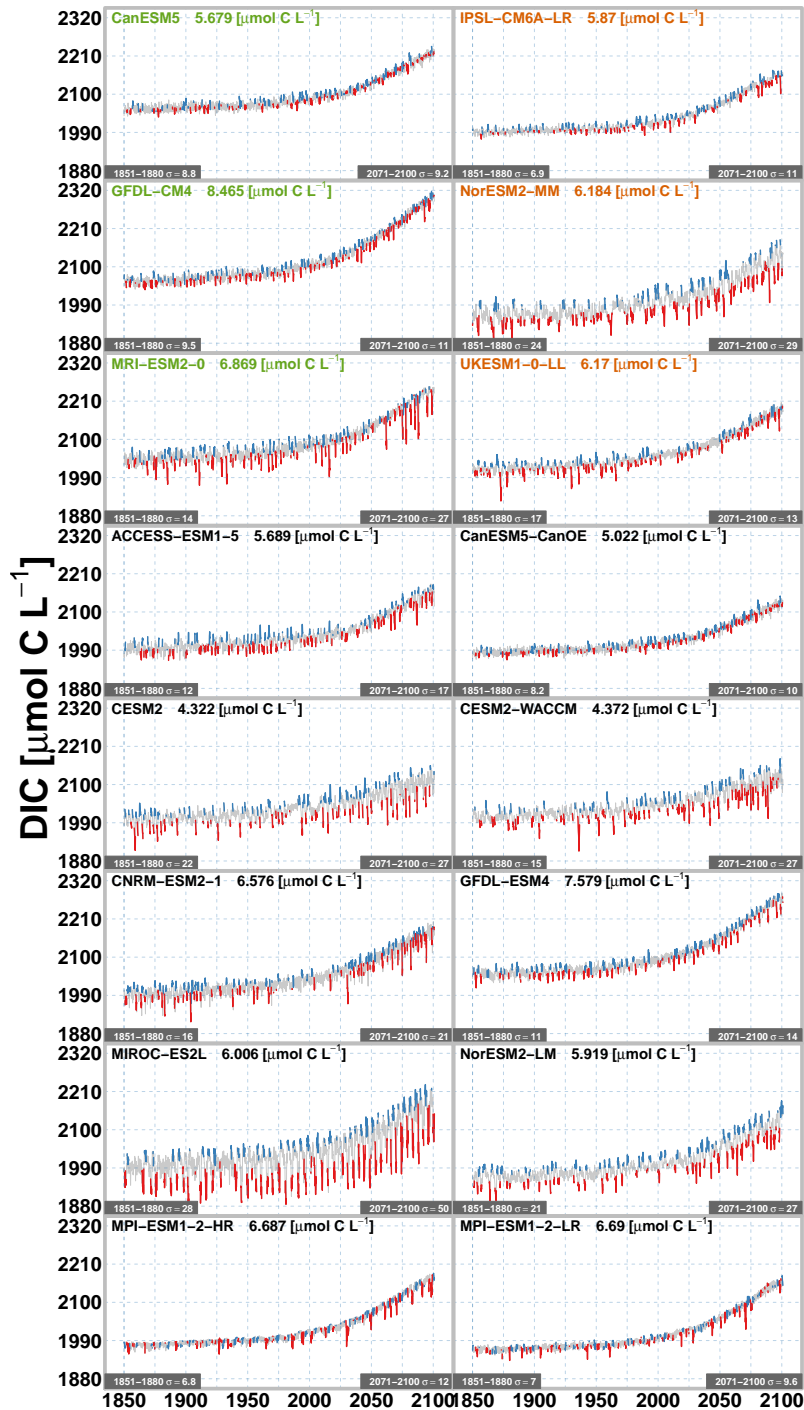


Figure S 14. Time-series of average surface DIC (in $\mu\text{mol C L}^{-1}$) from 1885 to 2100. The blue and red colours indicates the occurrence of the La Niña and El Niño regimes. The decadal trend is given for each model. Models names are given in green for selected models with shifting correlation sign, in orange for selected ones maintaining the negative correlation and black the others. The DIC standard deviation (σ) over the early historical (1851-1880) and future (2071-2100) periods are given for each model.